Assessment of metal-based dihydrofolate reductase inhibitors on a novel mesofluidic platform

Sarah A. P. Pereira[1], Lorenzo Biancalana[2], Fabio Marchetti[2], Paul J. Dyson[3], M. Lúcia M. F. S. Saraiva[1*]

[1] REQUIMTE, Departamento de Ciências Químicas, Faculdade de Farmácia, Universidade do Porto, Rua Jorge Viterbo Ferreira, nº 228, 4050-313 Porto, Portugal.

[2] Dipartimento di Chimica e Chimica Industriale Università di Pisa, Via G. Moruzzi 13, 56124 Pisa, Italy

[3] Institut des Sciences et Ingénierie Chimiques, École Polytechnique Fédérale de Lausanne (EPFL), 1015 Lausanne, Switzerland

[*] Corresponding author

E-mail address: lsaraiva@ff.up.pt

Tel.: +351 220428674; Fax: +351 226093483

Abstract

A new miniaturized micro sequential injection coupled with the lab-on-valve (μSIA–LOV) technique was full-blown to perform inhibitory studies on dihydrofolate reductase (DHFR). The system was used to evaluate the DHFR inhibition activity of metal-based anticancer compounds. The metal complexes exhibited IC_{50} values in the range 1.3 ± 0.3 to 108 ± 7 μM, with half of the complexes lying in the low μM range, i.e., 1.3 ± 0.3 to 4.4 ± 0.2 μM. For comparison, methotrexate (MTX), a known inhibitor of DHFR, has an IC_{50} value of 0.38 ± 0.06 μM. The μSIA–LOV is a versatile, robust, rapid, and easy to operate, allowing automated determination of DHFR inhibition. Moreover, the automated system requires very little sample (approximately 40 μL per analysis), uses minimal reagents (5 times less than the batch procedure used), and generates very little waste (around 1.2 mL per analysis) compared with batch methods, considerably reducing costs.

Keywords: miniaturization, μSIA–LOV, dihydrofolate reductase, metal complexes, inhibitory assays

1. Introduction

The third generation of flow analysis, also termed the lab-on-valve (LOV) concept, is an advanced mesofluidic approach that provides huge potential for instrumental miniaturization, automatization, and continuous monitoring of chemical and biochemical assays combined with automatic treatment of sample [1]. The LOV concept merges all the intrinsic benefits of flow methods with micro-flow injection analysis (μFIA) channels, using an integrated machined structure [2].

The resulting mesofluidic platform enables unattended chemical and biochemical analysis performance, independent of the matrix, chemistry, and samples involved, based on programmable pressure user-friendly software whose flow direction and rate are controlled [3].

Several detections could be associated with LOV platforms for several applications. There are some studies that reported the detection outside the LOV platform, using optic fibers that are connected to the flow cell [4] or also by chromatographic detection [5, 6]. On the other hand, there are others LOVs where the detection is inside the flow cell. This configuration is mainly used for absorbance detection but also for fluorimetry and chemiluminescence detection [7-10].

Micro sequential injection coupled to lab-on-valve (μSI-LOV) platform based on the programmable flow, has been used to perform biomolecular assays, including enzymatic assays [11, 12].

The study of enzyme kinetics allows both substrates and inhibitors to be characterized [13]. Standard enzyme kinetics studies typically employ manual bench techniques. However, the irregularity of the mixing time prior to detection and the time consumed by manual operation can lead to errors. Consequently, to improve accuracy and reduce the analysis time, LOV provides some advantages. The stopped-flow injection procedure has been successfully useful to the determination of reactions rate [14-16]. Basically, the flow can be stopped for a chosen period allowing the reaction to be continuously monitored as a function of time. Hence, we decided to develop a μSIA-LOV system with a new coupled detection module using optical fibers in 90º based on stopped-flow analysis to evaluate the ability of metal-based compounds to inhibit dihydrofolate reductase (DHFR).

DHFR enzyme catalyzes the reduction of dihydrofolate to tetrahydrofolate in an NADPH-dependent manner [17]. This enzymatic reaction interferes with the various

amino acids, thymidylate, and purines biosynthesis and is also an important target for anticancer drugs such as methotrexate. [18].

In recent years, significant efforts have been devoted to developing alternative metal-based drugs to platinum-based complexes currently extensively used to treat cancer [19-21]. One of the leading classes of compounds under intensive evaluation comprises ruthenium-arene complexes, which have been extensively evaluated in vivo and show highly promising properties [22]. Iron, due to its bioavailability, is another attractive element for a metal-based drug that noticeably decreases the toxic consequences of these compounds, and the chemical redox potential in physiological media, typically involving the oxidative states of Fe^{II} and Fe^{III}. Some monoiron complexes have been studied due to their anticancer effect and functionalized ferrocenes have emerged as promising candidates [23, 24]. Recently, different categories of diiron compounds based on the $\{Fe_2Cp_2(CO)_x\}$ scaffold (x = 2 or 3) have revealed potential in this field. They display ideal characteristics for a drug candidate, such as straightforward gram-scale synthesis from cheap precursors, generally noticeable water solubility, amphiphilicity, and wide structural variability by varying the substituents on the bridging hydrocarbyl ligand (i.e., hetero-carbyne or vinyliminium). These diiron complexes exhibit cytotoxicity against cancer cells ranging from low micromolar to inactive, and a marked selectivity towards noncancerous cells [25-27]. It has been outlined that aminocarbyne complexes probably exert their action by inhibition of thioredoxin reductase enzyme [25].

Herein, we describe a simple μSIA–LOV method for the automated determination of DHFR activity and its application to a selection of metal-based compounds with a previously established anticancer activity. Results of DHFR inhibition are discussed with respect to the structure and the antiproliferative activity of the compounds.

2. Materials and Methods

2.1. Reagents

Dihydrofolate reductase (DHFR), dihydrofolic acid (DFA), Nicotinamide adenine dinucleotide phosphate (NADPH), and methotrexate were purchased from Sigma. Dimethyl sulfoxide (DMSO) and ethanol were purchased from Merck and Fisher Chemical, respectively. Milli-Q water plus system was used to get ultrapure water with specific conductivity less than 0.1 μS cm^{-1}. This specific water was used to prepare all the solutions and the reagents were weighed in analytical grade.

The carrier solution used in the µSIA–LOV method was phosphate buffer solution (PBS) 0.1 mol L^{-1} at pH 7.4. DHFR, DFA, and NADPH were prepared every day in PBS 0.1 mol L^{-1} pH 7.4 at concentrations of 0.03 U, 0.74 mM, and 2.6 mM, respectively. These solutions were protected from light. DHFR and NADPH were incubated in an ice bath during the procedure.

Compounds **2a-d** [28], **3a** [29], **3b** [30], **4a-d** [25, 31], **5a-e** [26, 32], **6a-b** [33, 34] were synthesized as described in the literature. The compounds were dissolved in a DMSO solution diluted 10-fold with PBS 0.1 mol L^{-1} pH 7.4.

2.2. Flow and detection setup

The µSIA–LOV concept was developed with the purpose of improving the analytical performance since all the sample handling steps are integrated nearby to the measurement area. The developed system is represented in Figure 1. In Fig. S1 (supplementary material), it is presented the real image of this new LOV platform.

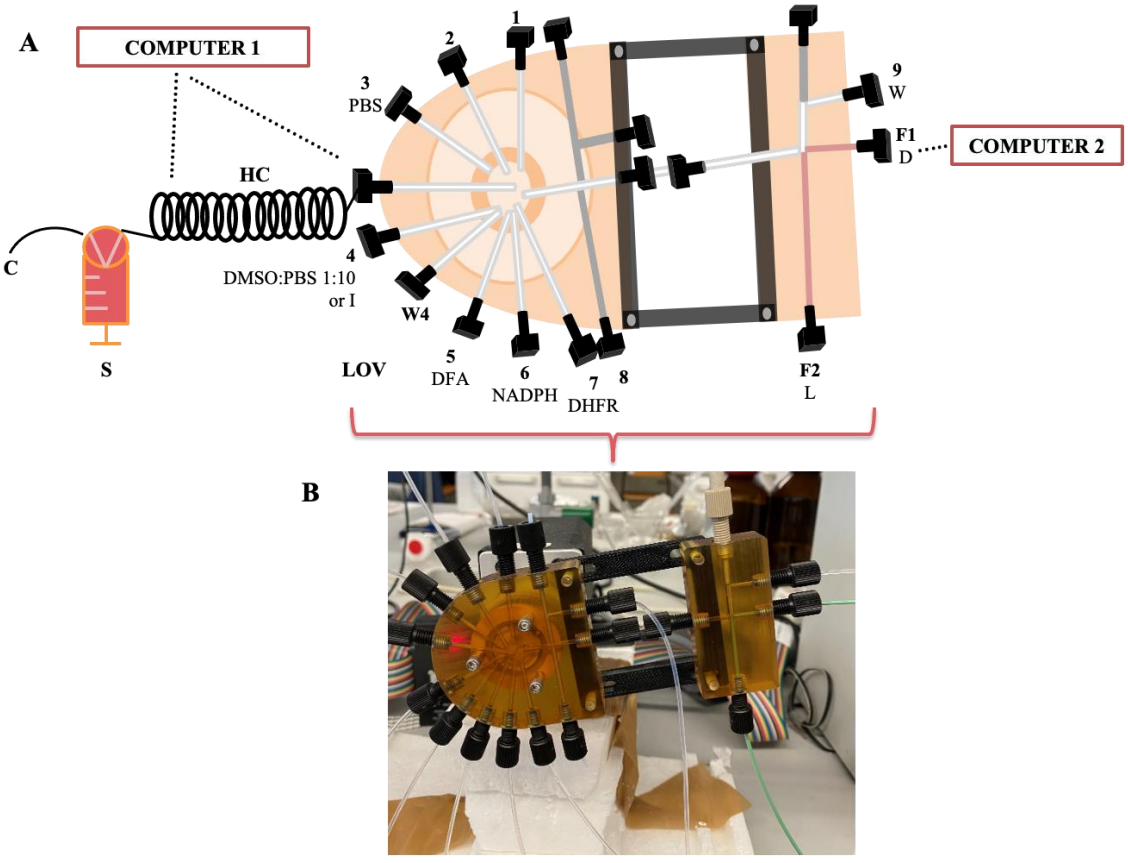

Figure 1 – A) Illustration of the µ-SIA LOV system used. C – Carrier; S – syringe; µSIA–LOV - micro sequential injection analysis coupled to lab-on-valve; HC – holding coil; DMSO: PBS - dimethylsulfoxide: phosphate buffer solution; I - inhibitor; PBS - phosphate buffer solution; DFA - dihydrofolic acid; NADPH - β-Nicotinamide adenine dinucleotide 2′-phosphate

reduced; DHFR - dihydrofolate reductase; W4 – waste of Port 4; F2 L - tungsten halogen lamp; F1 D - detector; W – waste. **B)** New LOV platform used in this work.

The flow manifold consisted of a microsyringe pump model Bu1S with the bi-directional flow (Crison Instruments S.A., Allela, Barcelona, Spain) with a 2500 μL syringe of gastight glass (Hamilton, Bonaduz, Switzerland) for programmed liquid handling; a holding coil with 2 m, a LOV platform fixed on the top of a ten-port multi-position selection valve that acts as a valve stator and two optical fibers, one with the light source and the other one with the optical detector. The central μSIA–LOV port is connected to the "out" position of the syringe pump. To fill the syringe with carrier solution it is necessary to move to the "in" position of the syringe pump. All system components are connected by PTFE tubing with 0.8 mm of internal diameter.
The valve position, flow direction, flow rate, duration of stop flow, the volumes of enzyme, sample, and substrate, as the acquirement and process of data analysis were controlled by a computer using MCF (Microsoft Foundation Classes) software.
To record the spectroscopic signals, it was used another computer with OOIBase32TM software version 2.0.6.5 of Ocean Optics. The decrease of NADPH was detected using an Ocean Optics USB4000 hand-held (from Ocean Optics Inc., Dunedin, FL, USA) which requires an optical detector for online photometric measurements and an LS-1-LL tungsten halogen light source (Ocean optics) that interfaces with the detector on the 3D LOV platform operating as an adaptive flow cell. For that, a couple of optical fibers with 600 μm of diameter were attached to the LOV platform and they were attached to the LOV platform in a 90º position to measure the fluorescent intensity of the reaction.

2.3. LOV analytical technique

Before starting the analyses of DHFR enzymatic inhibition in μSIA-LOV, it was confirmed the excitation and emission wavelengths of DHFR reaction. Thus, the excitation and emission wavelengths defined were, respectively, 357 nm and 472 nm. The inhibitory capacity of the compounds tested was determined by the inhibition percentages and half-maximal inhibitory concentration (IC_{50}) against DHFR enzyme using this automatic system. Previously, the syringe and the central tube of the selection valve were filled with the carrier solution (PBS 0.1 M at pH 7.4) and the selection valve adjacent tubes were filled with the reagents. The conduits at positions 3, 4, 5, 6, and 7

(see Figure 1) were filled with PBS pH 7.4, DMSO 10-fold diluted or test compound, DFA, NADPH, and DHFR, respectively. Afterward, the analytical cycle described in Table 1 was implemented by aspiration of 10 μL of DHFR, test compound, NADPH, DFA, and PBS (steps 1-5). Then, using flow reversal, the fluids were propelled to the flow cell (step 6) and the flow was stopped inside the flow cell for 90 seconds to acquire endlessly the reaction product fluorescence (step 7). After that, the detection cell was cleaned (step 8). To decrease the determination time, it was possible to repeat the analytical cycle twice without filling the syringe between determinations. All the determinations were led at room temperature and each assay was performed in triplicate.

Table 1 - μSIA-LOV analytical cycle defined to carry out the DHFR inhibition assays.

Step	**Position valve**	**Volume (μL)**	**Time (s)**	**Flow rate (mL min^{-1})**	**Event**
1	7	10	1.2	0.5	Aspiration of DHFR
2	4	10	1.2	0.5	Aspiration of inhibitor
3	6	10	1.2	0.5	Aspiration of NADPH
4	5	10	1.2	0.5	Aspiration of DFA
5	3	5	1.2	0.5	Aspiration of PBS
6	9	117	7	1	Propulsion to the flow cell
7	9	0	90	0	Stop period in flow cell
8	9	1000	60	1	Cleaning flow cell

2.4. Batch method

The activity of DHFR ($3.9x10^{-5}$ U) was evaluated fluorimetrically at 357/472 nm by measuring the reversible catalysis of NADPH-dependent reduction of DFA to tetrahydrofolic acid by DHFR (Figure 2) based on DHFR assay kit from Sigma-Aldrich, St. Louis, MO, USA. The assay contained 50 μM DFA and 60 μM NADPH in 0.1 M PBS (pH 7.4). The assays were led at room temperature considering the manufacturing specifications and each condition was performed in triplicate.

Figure 2 – DHFR enzymatic reaction.

3. Results and discussion

A μSIA-LOV system was developed for the automatic determination of DHFR activity and applied to a set of metal-based compounds with anticancer activity. DHFR catalyzed the reaction of dihydrofolate acid (DFA) with tetrahydrofolate (THF) using NADPH as a cofactor, and the fluorescence intensity (FI) of the reaction decreases as NADPH is concerted to $NADP^+$.

3.1. μSIA-LOV method optimization

The main parameters of the μSIA-LOV system, i.e., order of aspiration, the volume of the aliquots, propulsion time to the μSIA-LOV detector, reagents concentrations, and volume were studied (Table 2). Initially, the aspiration order of the reagent aliquots was studied and defined as DHFR – inhibitor - NADPH – DFA, since this aspiration order provides a 5 times higher analytical signal than the other conditions tested. In this case, the DHFR and NADPH will be close to the inhibitor aliquot (that will substitute the DMSO 10-fold diluted aliquot) and DFA has a lower system dilution as it is the last reagent to be aspirated. To further enhance the reagents mixture, the total volume of the reagent's aspiration was reduced to 40 μL, to decrease the reagents dispersion while preserving the low aspiration volumes without compromising the repeatability and the reliability of the assay.

Table 2 - Optimization conditions and results.

Parameters	Range	Values selected
Volume of reagents	5 µL – 10 µL	10 µL
Order of aspiration	DHFR - NADPH – inhibitor - DFA DFA – inhibitor - NADPH - DHFR DHFR – inhibitor - NADPH - DFA DFA - NADPH – inhibitor - DHFR	DHFR – inhibitor - NADPH - DFA
NADPH concentration	0.16 mM - 0.65 mM	0.32 mM
DHFR concentration	$9.8x10^{-5}$ U - $3.9x10^{-4}$ U	$2x10^{-4}$ U
DFA concentration	0.06 mM – 0.5 mM	0.09 mM
Volume propelled to the detector	85 µL - 135 µL	117 µL

In order to facilitate mixing of the aliquots to increase the reproducibility of the assay, the holding coil was placed near to the LOV platform. Since small reagent volumes are aspirated, these aliquots reach the holding coil (HC in Figure 1) in shapes of 8 which promotes better mixing and hence reaction. The propulsion time to the detector was also optimized towards obtain the best analytical signal in the detector. Comparing all the conditions tested, a propulsion time of 7 seconds provided the higher signal of NADPH in blank (15 times, 5 times and 3 times higher than 5.1 seconds, 6 seconds, and 8.1 seconds, respectively). All the propulsion times were tested with a flow rate of 1 mL min^{-1}.

After establishing the volume of the reagents zone, the concentrations of DHFR, DFA and NADPH were optimized. DHFR was studied in the concentration range $9.8x10^{-5}$ to $3.9x10^{-4}$ U (Unit - is described as a unit of enzyme activity that catalyse 1 µmol substrate conversion or the 1 µmol product formation in 1 min) [35]. An optimal DHFR concentration of $2x10^{-4}$ U was selected as direct proportionally with the FI is observed. The NADPH concentration (give range) was also optimized simultaneously with the DFA concentration (0.006 mM - 0.25 mM), with the NADPH concentration fixed at 0.32 mM.

Lastly, the concentration of DFA was then studied. The enzyme activity rate increases with increasing substrate concentration until the enzyme gets saturated with the substrate. A calibration curve was performed using the DFA concentration. The obtained calibration curve is F = (77.4 ± 60.7) C (mM) - (3.3 ± 4.1); R^2 = 0.99, where F corresponds to the intensity of fluorescence and C corresponds to the concentration of DFA in mM, with a confidence limit for the intercept and slope of 95%. The limit of detection and the limit of quantification is 0.01 mM and 1.07 mM, respectively.
The Michaelis-Menten constant (Km) and half of the maximal velocity (Vmax) were also calculated to be 0.25 mM and 10.76 mmol s^{-1}, respectively, using software GraphPad Prism 7. The concentration of substrate at which the enzymatic reaction rate is half of the maximal velocity (V_{max}) is Km. To guarantee the higher DHFR activity in the proposed inhibition assays, a 0.09 mM DFA concentration was defined.

3.2. Application of the µSIA-LOV system to determine metal-based compounds IC_{50} values

The outcome of diverse concentrations of each compound was evaluated in triplicate on the enzymatic activity using a 0.09 mM DFA solution which was selected from the linear concentration range of the calibration curve. In Fig. S2 of Supplementary material, it is represented the acquired polynomial relations including the normalized activity and each compound logarithm concentration. The whole compounds library tested inhibited DHFR in a dose-dependent manner and the IC_{50} values are presented in Table 3.

Table 3 - IC_{50} values of the compounds tested for DHFR inhibition.

Compound	Structure [a]	IC_{50} (µM ± SD)
1 Methotrexate	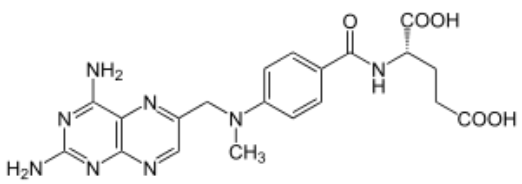	0.38 ± 0.06

2a **RAPTA-C**	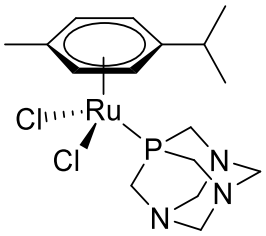	96.3 ± 7.5
2b **RAPTA-T**	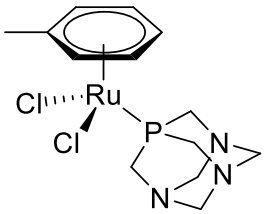	108 ± 7
2c **RAPTA-B**	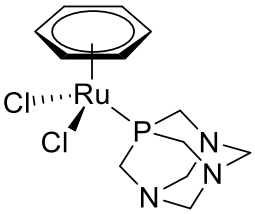	66.4 ± 9.7
2d **Oxali-RAPTA-C**	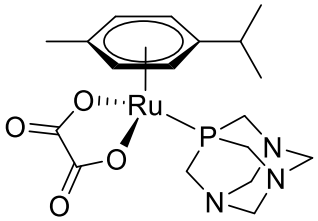	30.2 ± 1.6
3a **RUCYN**	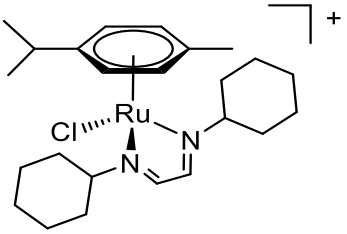	3.9 ± 0.8
3b	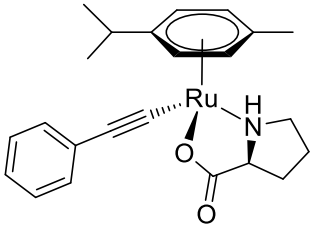	4.1 ± 0.9
4a	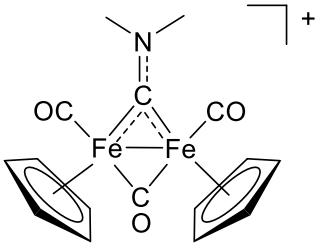	15.4 ± 4.8

4b	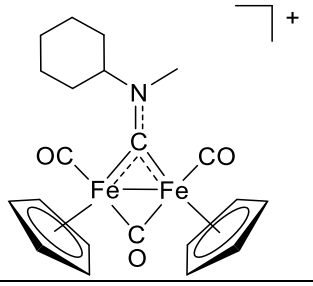	9.2 ± 3.5
4c	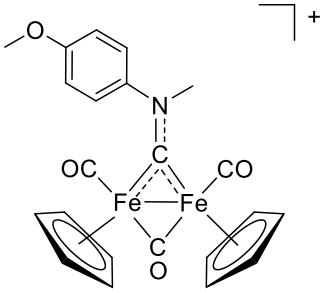	30.0 ± 1.9
4d	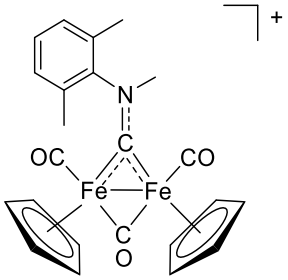	9.9 ± 0.1
5a	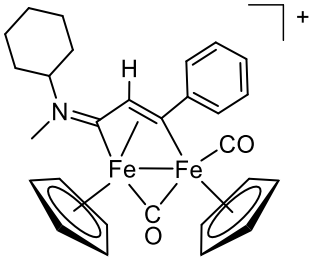	3.2 ± 0.5
5b	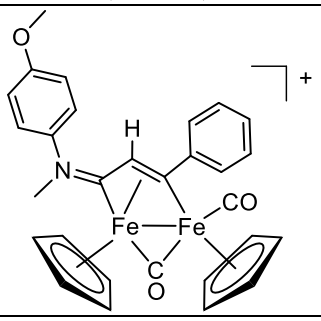	3.1± 0.1
5c	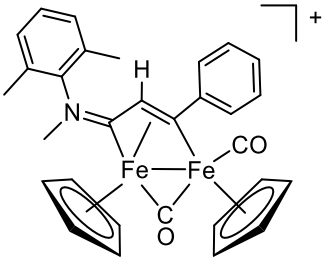	4.4 ± 0.2

5d	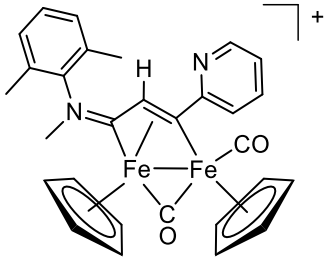	2.9 ± 0.2
5e	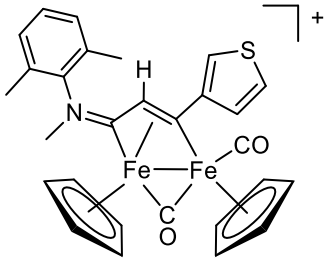	2.5 ± 0.2
6a	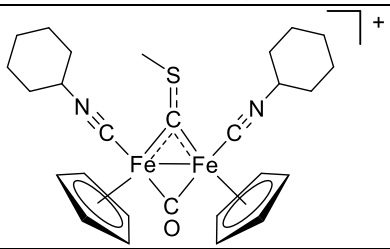	2.9 ± 0.4
6b	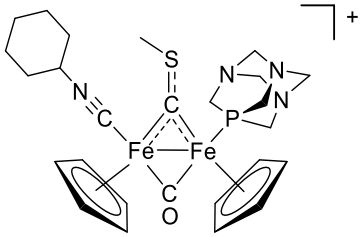	1.3 ± 0.3
7 Carboplatin	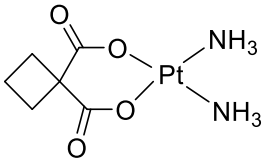	8.4 ± 0.8

[a] Cationic complexes as $CF_3SO_3^-$ salts, except **3a** (**RUCYN**) as NO_3^- salt.

Methotrexate (MTX) is a known DHFR inhibitor and was used as a positive control. In the literature, IC_{50} values for methotrexate vary with the type of assay performed. El-Naggar et al. evaluate the inhibition of DHFR enzyme using methotrexate and the in vitro IC_{50} obtained was 0.14 ± 1.38 μM [36] based on a different DHFR inhibition assay [37]. Abdelaziz et al. also determined the IC_{50} value of MTX by enzyme-linked immunosorbent assay (ELISA) technique and they obtained an IC_{50} value of 5.57 μM [38]. Using the μSIA-LOV system we obtained a IC_{50} of 0.38 ± 0.06 μM.

All the metal compounds tested were found to be less efficient DHFR inhibitors than methotrexate. Nevertheless, several complexes (**3a**, **5b**, **5c**, **5e**, **5f**, **6a** and **6b**) showed IC_{50} values in the low μM range, similar to that of their antiproliferative activity on

cancer cells (IC_{50} after 72 h incubation) [25, 26, 29, 31], indicating that DHFR inhibition might contribute to their antiproliferative mechanism.

The RAPTA derivatives (**2a-d**) showed a weak inhibitory activity, with IC_{50} values within the 30 to 100 μM range. These complexes are also exhibiting limited antiproliferative effects on cancer cells [39]. Conversely, the Ru(II) η^6-arene complex RUCYN (**3a**) was found to be a much more effective DHFR inhibitor (IC_{50} = 3.9 ± 0.8) and this compound is also cytotoxic to cancer cells. It is interesting to note that while RAPTA-C (and its derivatives) easily undergo Cl^- displacement in aqueous solution [40], and many protein adducts are known [41-43], RUCYN is comparatively inert in water and not particularly reactive with biosubstrates like Bovine Serum Albumin and Calf Thymus DNA [44].

Regarding diiron cyclopentadienyl complexes, the aminocarbyne derivatives (**4a-d**) showed moderate DHFR inhibition activity IC_{50} in the range 9 - 30 μM, whereas the vinyliminium **5a-f** and thiocarbyne **6a-b** complexes revealed the highest inhibitory properties against DHFR, with IC_{50} values all-around 3 μM, respectively. The higher effect provided by **4a** (IC_{50} = 15.4 ± 4.8 μM) compared to **4c** (IC_{50} = 30.0 ± 1.9) evidence that DHFR inhibition maybe not necessarily correlated with cytotoxicity, on considering that the former compound is inactive against various cancer cell lines, while the latter exerts considerable cytotoxicity even in 3D models [25]. With reference to vinyliminium complexes **5a-f**, the biological activity for DHFR inhibition, in comparison with cytotoxicity data [25, 26, 31, 32], is consistent within a given subset of compounds, and the influence of different substituents is minor. The widely used anticancer drug carboplatin was also evaluated and exhibits an IC_{50} value of 8.4 ± 0.8 μM, suggesting that DHFR inhibition may contribute, at least in part, to its anticancer effect.

3.3. Validation of μSIA-LOV

In order to validate our new approach to evaluate the inhibition of metal-based compounds using DHFR enzyme, some compounds were also analyzed using a batch method, with good agreement found between the two methods (see Table 4).

Table 4 - Assessment of μSIA-LOV and batch IC_{50} values.

Compounds	**IC_{50} μSIA-LOV ± SD (μM)**	**IC_{50} batch ± SD (μM)**
Methotrexate	0.38 ± 0.06	1.90 ± 0.07
4a	15.4 ± 4.8	17.6 ± 5.0
4b	9.2 ± 3.5	5.4 ± 0.5
4c	30.0 ± 1.9	30.5 ± 11.4
5b	3.2 ± 0.5	4.9 ± 0.6
6a	2.9 ± 0.4	5.4 ± 0.7

Three statistical tests were carried out to verify that the developed method is not statistically different from the batch method. In agreement with the student's t-test, the tabulated t value (2.57) was compared to the calculated t value (– 0.81). Comparing the results, there are no statistical differences at the confidence level of 95% [45]. It was also considered the p-value and considering the confidence level of 95% (p = 0.05), the p-value of 0.91 was obtained and, consequently, it confirmed the absence of statistical differences when both methods are compared. Also, a linear relationship was determined, and the equation was defined as:

IC_{50} LOV = (0.99 ± 0.29) IC_{50} BATCH - (0.64 ± 4.38)

where IC_{50}LOV and IC_{50}BATCH are, respectively, the IC_{50} results acquired in μSIA-LOV and batch methodologies with intercept and slope confidence limits of 95%. The expected intercept and slope values were not considerably different, respectively, from 0 and 1, therefore, it approves the agreement of μSIA-LOV and batch methodologies. Additionally, the coefficient of Pearson's correlation was considered (~ 0.96) validating the worthy correlation among both series of results obtained by batch and μSIA-LOV methods.

Comparing this new μSIA-LOV method with batch, in μSIA-LOV, the analytical signal is obtained in less than 3 minutes instead of the 5 minutes of the batch procedure. Furthermore, there is a significant reduction in solvents in the SIA system since we aspirated 5 times less of DHFR solution and 5 times less of NADPH and DFA solutions than in the batch method. In general, there is a decrease of 5 times in samples and

reagents consumed. Taking this into account and all the other advantages of μSIA-LOV, it is possible to obtain precise and reliable results using this new methodology.

4. Conclusions

A new automatic μSIA–LOV methodology was developed for the assessment of DHFR activity and used to determine the inhibitory effect of selected metal-based compounds endowed with anticancer activity. The μSIA–LOV system offers several advantages over batch methods, including a noteworthy reduction in reagents, solvents, and samples consumed and less operator involvement. Notably, the system was found to be suitable for routine analysis. The application of the μSIA–LOV method to study the inhibitory effect of a panel of metal-based anticancer compounds demonstrated that the inhibition of DHFR could be taken into consideration as a possible contribution to their antiproliferative activity.

Acknowledgments

The authors of this work acknowledged the financial support of the European Union (FEDER- European Fund for Regional Development funds POCI/01/0145/FEDER/007265) and National Funds (FCT/MEC, Fundação para a Ciência e Tecnologia e Ministério da Educação e Ciência) in the Partnership Agreement PT2020 UID/QUI/50006/2013. Moreover, we through POCI-01-0145-FEDER-030163, funded by FEDER through COMPETE 2020-Operational Program for Competitiveness and Internationalization (POCI), Portugal 2020. Sarah A. P. Pereira received a Ph.D. Grant (SFRH/BD/138835/2018) from FCT.

Declarations

Conflict of interest - The authors declare no competing interests.

Bibliography

[1] J. Ruzicka, Lab-on valve: Universal microflow analyzer based on sequential and bead injection, Analyst 125 (2000) 1053-1060.
[2] M. Miró, E.H. Hansen, Recent advances and future prospects of mesofluidic Lab-on-a-Valve platforms in analytical sciences – A critical review, Analytica Chimica Acta 750 (2012) 3-15.
[3] M. Miró, On-chip microsolid-phase extraction in a disposable sorbent format using mesofluidic platforms, TrAC Trends in Analytical Chemistry 62 (2014) 154-161.

[4] S.A.P. Pereira, F.D. Bobbink, P.J. Dyson, M.L.M.F.S. Saraiva, Automatic evaluation of cyclooxygenase 2 inhibition induced by metal-based anticancer compounds, J. Inorg. Biochem. 218 (2021) 111399.
[5] A.N. Ramdzan, L. Barreiros, M.I. Almeida, S.D. Kolev, M.A. Segundo, Determination of salivary cotinine through solid phase extraction using a bead-injection lab-on-valve approach hyphenated to hydrophilic interaction liquid chromatography, J Chromatogr A 1429 (2016) 284-91.
[6] M.S. Sammani, S. Clavijo, A. González, V. Cerdà, Development of an on-line lab-on-valve micro-solid phase extraction system coupled to liquid chromatography for the determination of flavonoids in citrus juices, Anal Chim Acta 1082 (2019) 56-65.
[7] Y. Wang, G. Yao, P. Zhu, X. Hu, Q. Xu, C. Yang, Lab-on-valve (LOV) system coupled to irreversible biamperometric detection for the on-line monitoring of catechol, Talanta 82(4) (2010) 1500-4.
[8] X. Chen, J. Wang, Z. Fang, A spectrophotometric procedure for DNA assay with a micro-sequential injection lab-on-valve meso-fluidic system, Talanta 67(1) (2005) 227-32.
[9] M.M. Grand, P. Chocholouš, J. Růžička, P. Solich, C.I. Measures, Determination of trace zinc in seawater by coupling solid phase extraction and fluorescence detection in the Lab-On-Valve format, Anal Chim Acta 923 (2016) 45-54.
[10] H. Oliveira, M. Grand, J. Ruzicka, C. Measures, Towards chemiluminescence detection in micro-sequential injection lab-on-valve format: A proof of concept based on the reaction between Fe(II) and luminol in seawater, Talanta 133 (2015) 107-11.
[11] D. Costa, M.L.C. Passos, A.M.O. Azevedo, M. Saraiva, Automatic evaluation of peroxidase activity using different substrates under a micro sequential injection analysis/lab-on-valve (mu SIA-LOV) format, Microchem J. 134 (2017) 98-103.
[12] S. Vidigal, I.V. Toth, A. Rangel, Sequential Injection Lab-on-Valve System for the Determination of the Activity of Peroxidase in Vegetables, J. Agric. Food Chem. 58(4) (2010) 2071-2075.
[13] S.K. Hartwell, K. Grudpan, Flow-Based Systems for Rapid and High-Precision Enzyme Kinetics Studies, Journal of Analytical Methods in Chemistry 2012 (2012) 450716.
[14] J.M. Hungerford, G.D. Christian, J. Ruzicka, J.C. Giddings, Reaction rate measurement by flow injection analysis using the gradient stopped-flow method, Analytical Chemistry 57(9) (1985) 1794-1798.
[15] K.S. Anderson, J.A. Sikorski, K.A. Johnson, Evaluation of 5-enolpyruvoylshikimate-3-phosphate synthase substrate and inhibitor binding by stopped-flow and equilibrium fluorescence measurements, Biochemistry 27(5) (1988) 1604-10.
[16] T. Kikas, A. Ivaska, Potentiometric measurements in sequential injection analysis lab-on-valve (SIA-LOV) flow-system, Talanta 71(1) (2007) 160-4.
[17] M.V. Raimondi, O. Randazzo, M. La Franca, G. Barone, E. Vignoni, D. Rossi, S. Collina, DHFR Inhibitors: Reading the Past for Discovering Novel Anticancer Agents, Molecules 24(6) (2019).
[18] A.S. Adesina, L.Y.P. Luk, R.K. Allemann, Cryo-kinetics Reveal Dynamic Effects on the Chemistry of Human Dihydrofolate Reductase, ChemBioChem n/a(n/a).
[19] W. Kaim, B. Schwederski, A. Klein, Bioinorganic Chemistry: Inorganic Elements in the Chemistry of Life, 2013.
[20] E. Boros, P.J. Dyson, G. Gasser, Classification of Metal-Based Drugs according to Their Mechanisms of Action, Chem 6(1) (2020) 41-60.

[21] E.J. Anthony, E.M. Bolitho, H.E. Bridgewater, O.W.L. Carter, J.M. Donnelly, C. Imberti, E.C. Lant, F. Lermyte, R.J. Needham, M. Palau, P.J. Sadler, H. Shi, F.-X. Wang, W.-Y. Zhang, Z. Zhang, Metallodrugs are unique: opportunities and challenges of discovery and development, Chemical Science 11(48) (2020) 12888-12917.
[22] M. Rausch, P.J. Dyson, P. Nowak-Sliwinska, Recent Considerations in the Application of RAPTA-C for Cancer Treatment and Perspectives for Its Combination with Immunotherapies, Advanced Therapeutics 2(9) (2019) 1900042.
[23] W.A. Wani, U. Baig, S. Shreaz, R.A. Shiekh, P.F. Iqbal, E. Jameel, A. Ahmad, S.H. Mohd-Setapar, M. Mushtaque, L. Ting Hun, Recent advances in iron complexes as potential anticancer agents, New Journal of Chemistry 40(2) (2016) 1063-1090.
[24] U. Basu, M. Roy, A.R. Chakravarty, Recent advances in the chemistry of iron-based chemotherapeutic agents, Coordination Chemistry Reviews 417 (2020) 213339.
[25] L. Biancalana, M. De Franco, G. Ciancaleoni, S. Zacchini, G. Pampaloni, V. Gandin, F. Marchetti, Easily Available, Amphiphilic Diiron Cyclopentadienyl Complexes Exhibit in Vitro Anticancer Activity in 2D and 3D Human Cancer Cells through Redox Modulation Triggered by CO Release, Chemistry – A European Journal 27(39) (2021) 10169-10185.
[26] S. Braccini, G. Rizzi, L. Biancalana, A. Pratesi, S. Zacchini, G. Pampaloni, F. Chiellini, F. Marchetti, Anticancer Diiron Vinyliminium Complexes: A Structure–Activity Relationship Study, Pharmaceutics 13(8) (2021) 1158.
[27] D. Rocco, L.K. Batchelor, G. Agonigi, S. Braccini, F. Chiellini, S. Schoch, T. Biver, T. Funaioli, S. Zacchini, L. Biancalana, M. Ruggeri, G. Pampaloni, P.J. Dyson, F. Marchetti, Anticancer Potential of Diiron Vinyliminium Complexes, Chemistry 25(65) (2019) 14739.
[28] C. Scolaro, A. Bergamo, L. Brescacin, R. Delfino, M. Cocchietto, G. Laurenczy, T.J. Geldbach, G. Sava, P.J. Dyson, In Vitro and in Vivo Evaluation of Ruthenium(II)−Arene PTA Complexes, Journal of Medicinal Chemistry 48(12) (2005) 4161-4171.
[29] L. Biancalana, L.K. Batchelor, T. Funaioli, S. Zacchini, M. Bortoluzzi, G. Pampaloni, P.J. Dyson, F. Marchetti, α-Diimines as Versatile, Derivatizable Ligands in Ruthenium(II) p-Cymene Anticancer Complexes, Inorganic Chemistry 57(11) (2018) 6669-6685.
[30] D. Carmona, C. Vega, F.J. Lahoz, R. Atencio, L.A. Oro, M.P. Lamata, F. Viguri, E. San José, Synthesis and Stereochemistry of Half-Sandwich Alkynyl Amino Acidate Complexes of Rhodium(III), Iridium(III), and Ruthenium(II), Organometallics 19(12) (2000) 2273-2280.
[31] G. Agonigi, L. Biancalana, M.G. Lupo, M. Montopoli, N. Ferri, S. Zacchini, F. Binacchi, T. Biver, B. Campanella, G. Pampaloni, V. Zanotti, F. Marchetti, Exploring the Anticancer Potential of Diiron Bis-cyclopentadienyl Complexes with Bridging Hydrocarbyl Ligands: Behavior in Aqueous Media and In Vitro Cytotoxicity, Organometallics 39(5) (2020) 645-657.
[32] D. Rocco, L.K. Batchelor, G. Agonigi, S. Braccini, F. Chiellini, S. Schoch, T. Biver, T. Funaioli, S. Zacchini, L. Biancalana, M. Ruggeri, G. Pampaloni, P.J. Dyson, F. Marchetti, Anticancer Potential of Diiron Vinyliminium Complexes, Chemistry – A European Journal 25(65) (2019) 14801-14816.
[33] N.C. Schroeder, R. Funchess, R.A. Jacobson, R.J. Angelici, Reactions of Cp2Fe2(CO)2(.mu.-CO)(.mu.-CSR)+ bridging-carbyne complexes with nucleophiles, Organometallics 8(2) (1989) 521-529.

[34] F. Marchetti, S. Zacchini, V. Zanotti, C–N Coupling of Isocyanide Ligands Promoted by Acetylide Addition to Diiron Aminocarbyne Complexes, Organometallics 34(14) (2015) 3658-3664.
[35] R. Eisenthdal, M.J. Danson, Enzyme assays - a practical approach, 2002.
[36] M. El-Naggar, H.A. Sallam, S.S. Shaban, S.S. Abdel-Wahab, A.E.-G. E Amr, M.E. Azab, E.S. Nossier, M.A. Al-Omar, Design, Synthesis, and Molecular Docking Study of Novel Heterocycles Incorporating 1,3,4-Thiadiazole Moiety as Potential Antimicrobial and Anticancer Agents, Molecules (Basel, Switzerland) 24(6) (2019) 1066.
[37] R. PIGNATELLO, G. SPAMPINATO, V. SORRENTI, L. VICARI, C. DI GIACOMO, A. VANELLA, G. PUGLISI, Aliphatic α,γ-bis(Amides) of Methotrexate. Influence of Chain Length on In-vitro Activity Against Sensitive and Resistant Tumour Cells, Pharmacy and Pharmacology Communications 5(4) (1999) 299-305.
[38] O.A. Abdelaziz, W.M. El Husseiny, K.B. Selim, H.M. Eisa, Dihydrofolate reductase inhibition effect of 5-substituted pyrido[2,3-d]pyrimidines: Synthesis, antitumor activity and molecular modeling study, Bioorganic Chemistry 90 (2019) 103076.
[39] B.S. Murray, M.V. Babak, C.G. Hartinger, P.J. Dyson, The development of RAPTA compounds for the treatment of tumors, Elsevier Science Sa, 2016, pp. 86-114-86-114.
[40] C. Scolaro, C.G. Hartinger, C.S. Allardyce, B.K. Keppler, P.J. Dyson, Hydrolysis study of the bifunctional antitumour compound RAPTA-C, [Ru(η6-p-cymene)Cl2(pta)], J. Inorg. Biochem. 102(9) (2008) 1743-1748.
[41] M. Groessl, M. Terenghi, A. Casini, L. Elviri, R. Lobinski, P.J. Dyson, Reactivity of anticancer metallodrugs with serum proteins: new insights from size exclusion chromatography-ICP-MS and ESI-MS, Journal of Analytical Atomic Spectrometry 25(3) (2010) 305-313.
[42] Z. Adhireksan, G.E. Davey, P. Campomanes, M. Groessl, C.M. Clavel, H. Yu, A.A. Nazarov, C.H.F. Yeo, W.H. Ang, P. Dröge, U. Rothlisberger, P.J. Dyson, C.A. Davey, Ligand substitutions between ruthenium–cymene compounds can control protein versus DNA targeting and anticancer activity, Nature Communications 5(1) (2014) 3462.
[43] B. Wu, M.S. Ong, M. Groessl, Z. Adhireksan, C.G. Hartinger, P.J. Dyson, C.A. Davey, A Ruthenium Antimetastasis Agent Forms Specific Histone Protein Adducts in the Nucleosome Core, Chemistry – A European Journal 17(13) (2011) 3562-3566.
[44] E. Zanda, N. Busto, L. Biancalana, S. Zacchini, T. Biver, B. Garcia, F. Marchetti, Anticancer and antibacterial potential of robust Ruthenium(II) arene complexes regulated by choice of α-diimine and halide ligands, Chemico-Biological Interactions 344 (2021) 109522.
[45] J.C. Miller, J.N. Miller, Estadística para Química Analítica, in: A.W. Ibroamerican (Ed.) Wilmington, USA, 1993.

Supplementary material

Figure S1 – Experimental inhibition data of tested compounds in the DHFR inhibition assays.

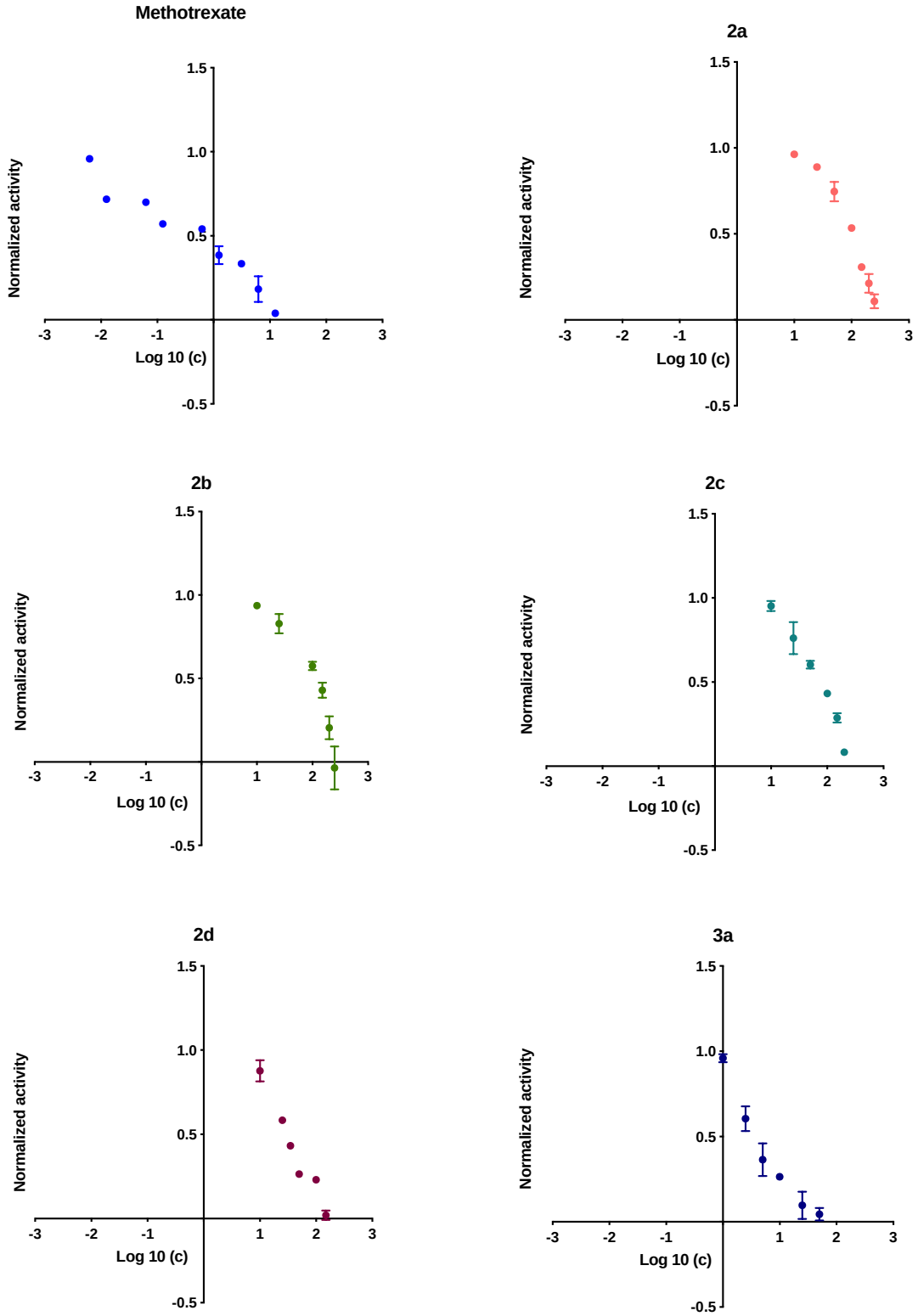

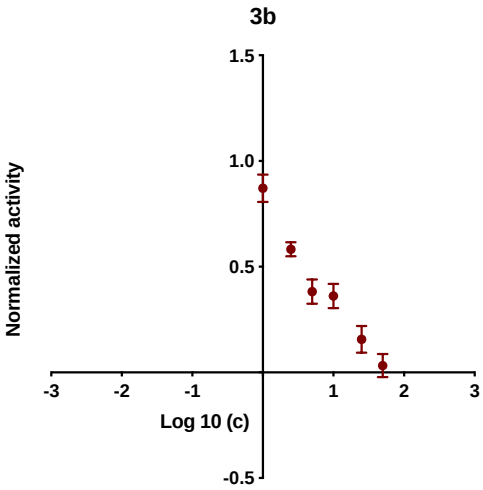
3b
Normalized activity
1.5
1.0
0.5
-0.5
-3
-2
-1
1
2
3
Log 10 (c)

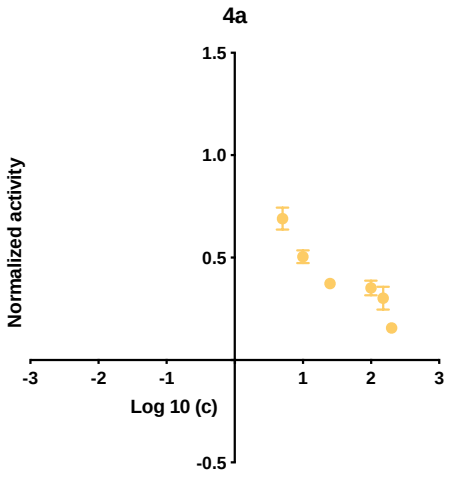
4a
Normalized activity
1.5
1.0
0.5
-0.5
-3
-2
-1
1
2
3
Log 10 (c)

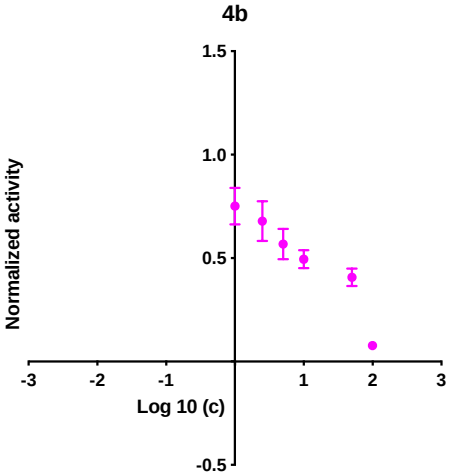
4b
Normalized activity
1.5
1.0
0.5
-0.5
-3
-2
-1
1
2
3
Log 10 (c)

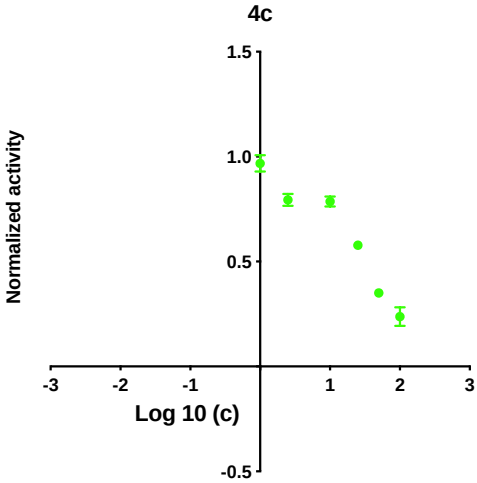
4c
Normalized activity
1.5
1.0
0.5
-0.5
-3
-2
-1
1
2
3
Log 10 (c)

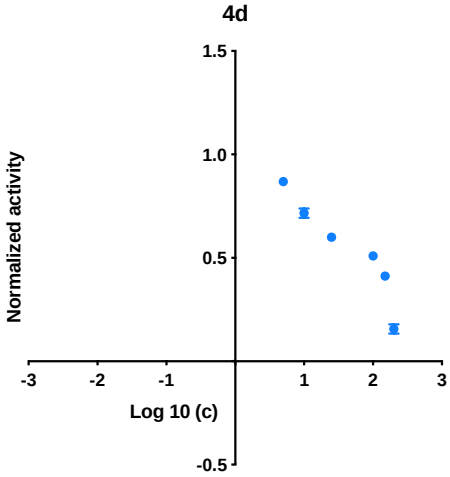
4d
Normalized activity
1.5
1.0
0.5
-0.5
-3
-2
-1
1
2
3
Log 10 (c)

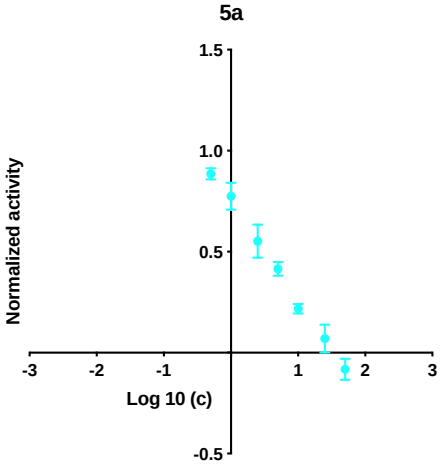
5a
Normalized activity
1.5
1.0
0.5
-0.5
-3
-2
-1
1
2
3
Log 10 (c)

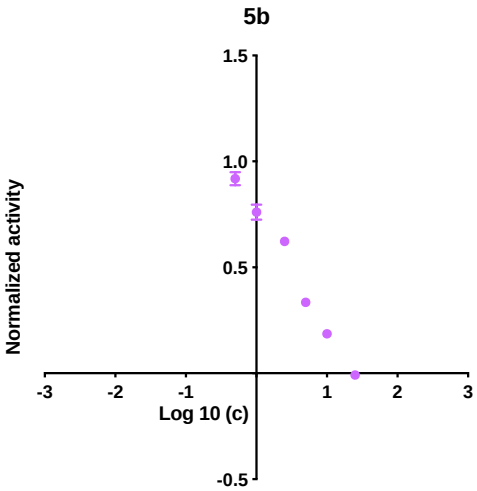
5b
Normalized activity
1.5
1.0
0.5
-0.5
-3
-2
-1
1
2
3
Log 10 (c)

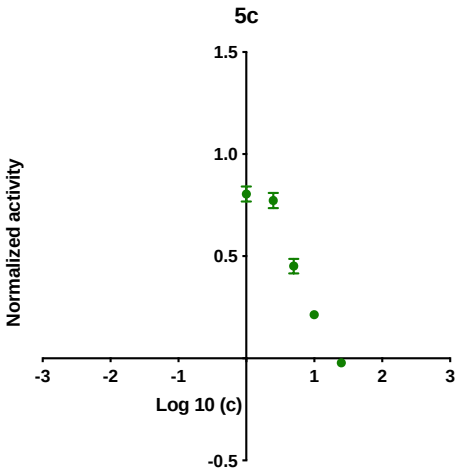
5c
Normalized activity
1.5
1.0
0.5
-0.5
-3
-2
-1
1
2
3
Log 10 (c)

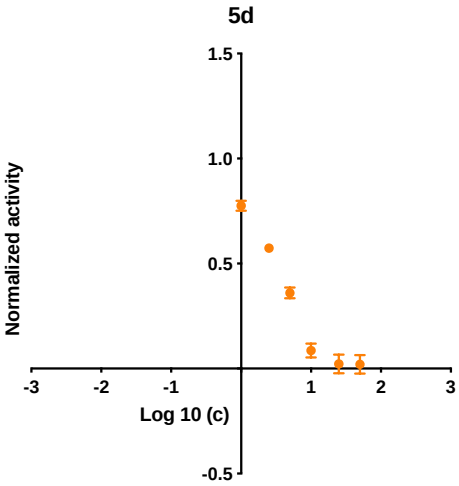
5d
Normalized activity
1.5
1.0
0.5
-0.5
-3
-2
-1
1
2
3
Log 10 (c)

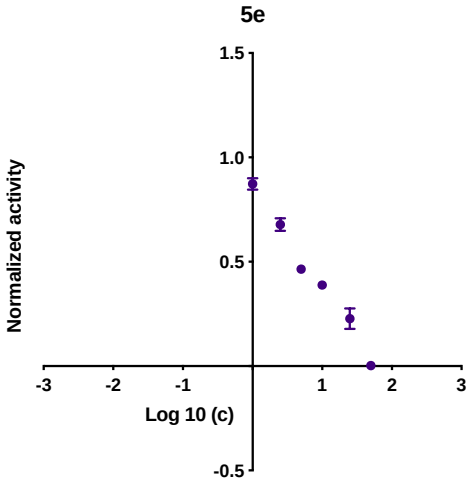
5e
Normalized activity
1.5
1.0
0.5
-0.5
-3
-2
-1
1
2
3
Log 10 (c)

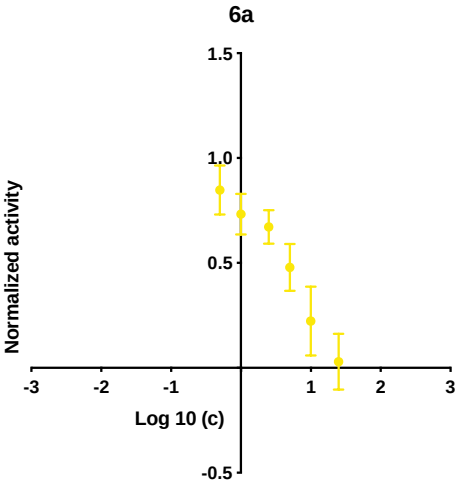
6a
Normalized activity
1.5
1.0
0.5
-0.5
-3
-2
-1
1
2
3
Log 10 (c)

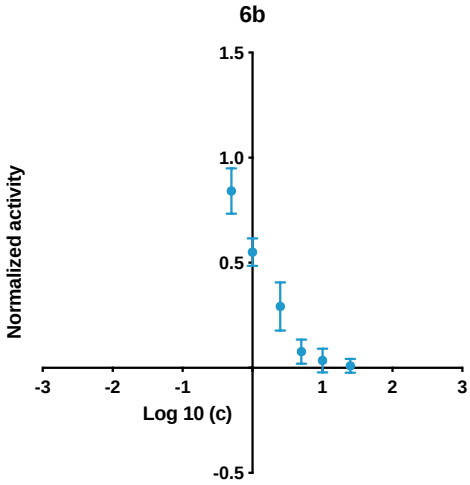
6b
Normalized activity
1.5
1.0
0.5
-0.5
-3
-2
-1
1
2
3
Log 10 (c)

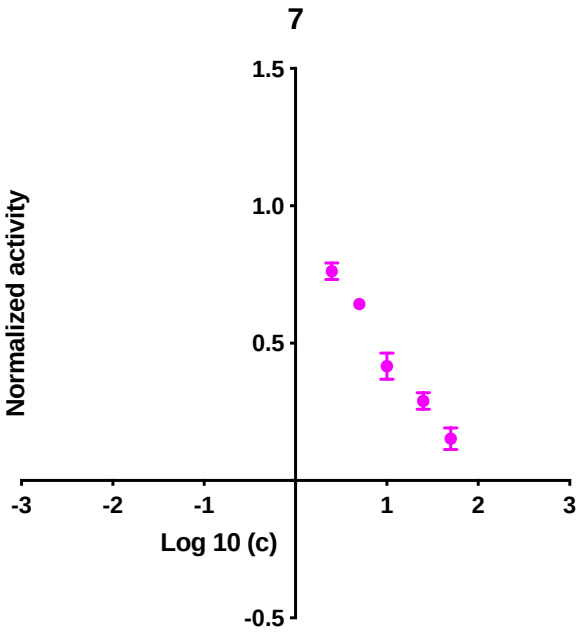
7
1.5
1.0
0.5
-0.5
Normalized activity
-3
-2
-1
1
2
3
Log 10 (c)